Revisiting the Definition of the Drag Coefficient in the Marine Atmospheric Boundary Layer

RICHARD J. FOREMAN AND STEFAN EMEIS

Institute for Meteorology and Climate Research, Karlsruhe Institute of Technology, Garmisch-Partenkirchen, Germany

(Manuscript received 24 December 2009, in final form 15 June 2010)

ABSTRACT

A new functional form of the neutral drag coefficient for moderate to high wind speeds in the marine atmospheric boundary layer for a range of field measurements as reported in the literature is proposed. This new form is found to describe a wide variety of measurements recorded in the open ocean, coast, fetch-limited seas, and lakes, with almost one and the same set of parameters. This is the result of a reanalysis of the definition of the drag coefficient in the marine boundary layer, which finds that a constant is missing from the traditional definition of the drag coefficient. The constant arises because the neutral friction velocity over water surfaces is not directly proportional to the 10-m wind speed, a consequence of the transition to rough flow at low wind speeds. Within the rough flow regime, the neutral friction velocity is linearly dependent on the 10-m wind speed; consequently, within this rough regime, the new definition of the drag coefficient is not a function of the wind speed. The magnitude of the new definition of the neutral drag coefficient represents an upper limit to the magnitude of the traditional definition.

1. Introduction

Despite conflicting evidence in the past (Garratt 1977), it is now accepted that the drag coefficient (defined below) in the marine atmospheric boundary layer (MABL) is an increasing function of the wind speed (Sullivan and McWilliams 2010) for moderate wind speeds. At higher wind speeds, however, recent evidence suggests that the drag coefficient tends toward a constant value (Donelan et al. 2004; Black et al. 2007). The exact equation that describes the relationship between the drag coefficient and wind speed is dependent on the author (Geernaert 1990). Although a universal consensus does not exist, the most widely cited relationships are possibly those proposed by Smith (1980), Large and Pond (1981), Yelland et al. (1998), and in particular the Coupled Ocean–Atmosphere Response Experiment (COARE) algorithm (Fairall et al. 1996, 2003).

It is thought that differences in measured drag coefficients between independent studies are a function of the state of the sea (Donelan 1990). Attempts over the years to explain these differences have led to the use of various conceptual tools such as the wave steepness or slope (e.g., Hsu 1974) and wave age (e.g., Maat et al. 1991). For example, the drag coefficient is thought to increase with younger waves (decreasing wave age) (Smith et al. 1992). The precise dependence of the drag coefficient on one or more of these tools is an ongoing area of research in air–sea interaction (Sullivan and McWilliams 2010).

However, our intention here is not to review these tools but rather to take a step back and revisit the definition of the drag coefficient, to investigate whether the definition of the drag coefficient in the MABL is consistent with observations over the past 35 years, and to determine whether an alternative approach could help describe these observations. Summaries of measurements and the state of knowledge prior to approximately 1975 can be found in Wu (1980) and Garratt (1977).

For the purposes of this study, data previously reported in the literature is collected and reanalyzed. The choice of data is limited to what can be readily accessed and that spans a sufficient velocity range, the reason for which will be clear below. This includes data reported in tabulated form (e.g., Smith 1980) or in a figure whereby data points can be clearly extracted (e.g., Drennan et al. 2003).

The structure of this paper is as follows: An initial analysis of the standard definition of the drag coefficient

Corresponding author address: Richard J. Foreman, Karlsruhe Institute of Technology, Kreuzeckbahnstrasse 19, Garmisch-Partenkirchen 82467, Germany.
E-mail: richard.foreman@kit.edu

DOI: 10.1175/2010JPO4420.1

is conducted and compared against a wide collection of data as sourced from the literature. Based on this analysis, a new definition of the drag coefficient in the MABL is proposed that fits a wide range of reported data, under a range of field conditions. The new drag coefficient is then related to the old. Finally, an explanation is offered for data that appear to fit the new definition less well.

2. Analysis

a. Definition of the neutral drag coefficient

The neutral drag coefficient is defined as a squared ratio of the friction velocity u_* to a wind speed usually reported at a 10-m height, U_{10}, where

$$C_D = \frac{u_*^2}{U_{10}^2}. \tag{1}$$

Figure 1 shows the neutral drag coefficient as calculated from sources listed in Table 1, where the lines representing Eq. (14) and $C_D = 0.0026$ are explained below. It is assumed here that the data listed in Table 1 has been corrected for neutral conditions. Data uncorrected for stability will deviate from the true magnitude of C_D as defined by Eq. (1) (Smith 1980). Details of the data displayed in Fig. 1 can be found in Table 1, and an explanation of the various parameters in Table 1 follows.

Figure 1 shows that, except for low velocities, C_D is an increasing function of U_{10}, until roughly 20 m s^{-1} when C_D appears to level off. Highlighted in Fig. 1 are the Humidity Exchange over the Sea (HEXOS) results (triangles) as reported by Janssen (1997), which do not display this leveling off, whereas those of Anderson (1993) do (squares). An increasing C_D with U_{10} is generally thought to be a consequence of increasing surface roughness with increasing wind velocity (Charnock 1955; Smith 1988; Hasse and Smith 1997; Fairall et al. 1996, 2003).

The standard definition of the drag coefficient assumes that u_* is directly proportional to U_{10}. This is evident upon rearranging Eq. (1) whereby

$$u_* = (C_D^{1/2})U_{10}, \tag{2}$$

and the square root of the drag coefficient must be the slope of a plot of u_* against U_{10}. Displayed in Fig. 2 is such a plot using data from the sources listed in Table 1 where for higher velocities it can be seen that u_* is approximately linearly dependent on U_{10}. The linear dependence of u_* on U_{10} is precisely what is assumed in Eq. (2). Why, therefore, is the drag coefficient as presented in Fig. 1 not constant within the apparent linear regime?

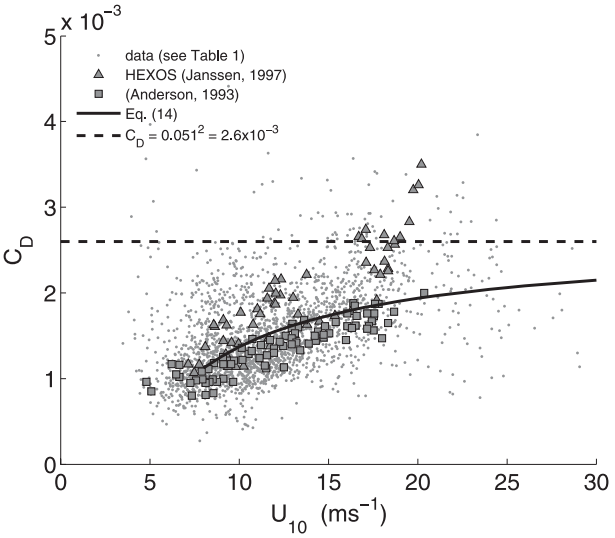

FIG. 1. The neutral drag coefficient plotted as a function of the 10-m wind speed for data listed in Table 1. Triangles represent the HEXOS data (Janssen 1997) and squares are data reported by Anderson (1993). Equation (14) is explained in the text, as well as the horizontal line, where $C_D = 0.0026$.

The answer to this question can be found once more from Fig. 2, where a straight line is fitted to an apparent linear regime. Figure 2 shows that while u_* is proportional to U_{10}, u_* is not directly proportional to U_{10}, and this information is masked if one merely views a plot displaying $C_D = f(U_{10})$. The linear equation describing that in Fig. 2 is

$$u_* = 0.051U_{10} - 0.14, \tag{3}$$

and hence a constant must be inserted into the usual definition of the drag coefficient such that now

$$u_* = C_m U + b, \tag{4}$$

where b is a constant that must have dimensions of meters per second in order for Eq. (4) to be dimensionally consistent. All measurements combined, as shown in Fig. 2, give $b = -0.14$ m s^{-1} for $U_{10} \geq 8$ m s^{-1} and $u_* \geq 0.27$ m s^{-1}, where justification for these numbers is provided in the following section. Here, the drag coefficient has been relabeled to distinguish it from the traditional definition.

The HEXOS results have been highlighted in Fig. 2 since they are noticeably nonlinear. A nonlinear dependence of u_* on U_{10} has also been spotted by Davidson (1974) and Oost et al. (2002). However, they considered u_* for the full range of U_{10}, whereas below we will show that linearity is constrained to higher velocities. A possible reason for nonlinearity for higher velocities will be

given further below where the nonlinearity is also quantified, since some datasets are clearly more nonlinear than others. For example, the data reported by Anderson (1993), also displayed in Fig. 2, is more linear than the HEXOS results reported by Janssen (1997).

b. Formulation of a new drag coefficient

In contrast to what has been illustrated above for flows over water, flows over a typically rough terrain exhibit a near-direct linear proportionality between the friction velocity and the wind speed; that is, b is small and can be neglected [e.g., see Fig. 1 in Hicks (1976) and the bottom of Table 1 here]. While aerodynamically rough flow exists even at low velocities over land, this may not be true over water, because the roughness length over water surfaces is smoother by one or two orders of magnitude compared with land surfaces (Stull 1988). It could be possible therefore that at low velocities, that is, in the nonlinear, low velocity regime, the flow in the marine surface layer may not be completely aerodynamically rough but rather within a smooth or transition flow regime. In correspondence with measurements showing linearity in clearly rough flows over land, it will be shown here that the existence of the approximately linear regime of u_* with U_{10} corresponds to the regime of aerodynamically rough flow over water as it does over land. To show this, however, we must first reject data outside the rough flow regime in flows over water.

A surface layer flow can be classified as aerodynamically rough as long as the roughness Reynolds number [Lange et al. (2004) gives a nice summary of the origins of this parameter]

$$R_f = \frac{u_* z_o}{\nu} > 2.3, \tag{5}$$

where ν is the kinematic viscosity. With Charnock's relation (Charnock 1955) providing an expression for the roughness height,

$$z_o = \frac{\alpha u_*^2}{g}, \tag{6}$$

a friction velocity can be found where

$$u_{*_o} = \left(\frac{2.3\nu g}{\alpha}\right)^{1/3} \tag{7}$$

and can be said to equal the friction velocity at the onset of aerodynamically rough flow. To show that a linear relationship between the friction velocity and wind speed exists over water within the rough flow regime, all data for $u_* \le u_{*_o}$ must be rejected. However, the exact magnitude of u_{*_o} is uncertain owing to the uncertainty of α (see below) and possibly also R_f. Therefore, an iterative procedure to solve for Eq. (7) is needed, which also involves the stipulation of a minimum value U_o for the 10-m wind speed U_{10}.

Recalling that, if the drag coefficient has the general form [recall Eq. (4)]

$$u_* = C_m U_{10} + b, \tag{8}$$

then $u_*(U_{10} = U_o) = u_{*_o}$ and thus

$$u_{*_o} = U_o C_m + b, \tag{9}$$

where it can be seen that the assumed linear relationship between the friction velocity and the wind speed also gives a relationship between u_{*_o} and U_o. This also gives an expression for the constant b, where

$$b = \left(\frac{2.3\nu g}{\alpha}\right)^{1/3} - U_o C_m. \tag{10}$$

A new definition of the drag coefficient is then obtained if Eq. (10) is substituted back into our original definition, Eq. (8), to give

$$u_* = C_m(U_{10} - U_o) + \left(\frac{2.3\nu g}{\alpha}\right)^{1/3}, \tag{11}$$

provided that both $u_* \ge u_{*_o}$ and $U_{10} \ge U_o$; to find these values, the following iterative approach is adopted:

(i) U_o is assumed;
(ii) linear regression coefficients C_m and b for $U_{10} \ge U_o$ are calculated;
(iii) u_{*_o} can then be calculated from C_m and b via Eq. (9);
(iv) C_m and b are then recalculated for $u_* \ge u_{*_o}$;
(v) steps (iii) and (iv) are repeated until the numbers converge; and
(vi) α can then be found from Eq. (7).

Plotted in Fig. 3 is α as calculated from Eq. (7) based on a number of assumed values of U_o and shows that $\alpha = 0.018$ (and hence $u_{*_o} = 0.27\ \mathrm{m\ s^{-1}}$) corresponds to $U_o = 8\ \mathrm{m\ s^{-1}}$. Substituting these values into Eq. (11) gives

$$u_* = C_m(U_{10} - 8) + 0.27 \quad \text{for} \quad U_{10} \ge 8, u_* \ge 0.27\,\mathrm{m\,s^{-1}}, \tag{12}$$

with $C_m = 0.051$. For the purposes of calculating C_m for each individual dataset (Table 1), data below $U_{10} = 8\ \mathrm{m\ s^{-1}}$ and $u_* = 0.27\ \mathrm{m\ s^{-1}}$ have been neglected. In this way, it can be seen that values for C_m, as determined from a range of reported data using different techniques in various locations, give a standard deviation (=0.006)

TABLE 1. Relevant parameters as determined from previously published data. All data are based on a 10-m standard height except where noted: C_m is the new drag coefficient in the MABL, b is the neglected constant in the traditional definition of C_D, and u_{*_o} is the friction velocity at the onset of aerodynamically rough flow. In the determination of these linear regression coefficients, data below $U_{10} = 8$ m s^{-1} and $u_* = 0.27$ m s^{-1} have been neglected. The correlation coefficient (Corr coef) is taken as that between the u_* and U_{10} distribution. The value R_{ns} is described further in the text and is the ratio of the norm of residuals as found from a linear and quadratic fit to data [see Eq. (21)]. A negative sign leading this value (−) here denotes a quadratic model that is concave down.

Author	C_m	$-b$ (m s^{-1})	u_{*_o} (m s^{-1})	Corr coef	R_{ns}	ΔU_{10}[a] (m s^{-1})	Location	Method[b]	Data source[c]
Avg (over all data)	0.051	0.14	0.27	0.93	(−)1.000[d]	8–30	—	—	—
Open ocean									
Large and Pond (1982)	0.048	0.14	0.24	0.97	0.982	8–18	North Pacific [Storm Transfer and Response Experiments (STREX)]	PV, ID	Fig. 8b
Banner et al. (1999)	0.052	0.13	0.29	0.84	0.988	8–20	Southwest Tasmania [Southern Ocean Waves Experiment (SOWEX)]	A, ECA	Table 2
Persson et al. (2005)	0.057	0.18	0.27	0.86	0.969	8–20	Mid-Atlantic [Fronts and Atlantic Storm Track Experiment (FASTEX)]	S, ECM	Fig. 7a[e]
Black et al. (2007)	0.047	0.12	0.25	0.87	(−)0.993	10–29	Atlantic [Coupled Boundary Layer Air–Sea Transfer (CBLAST)]	A, ECA	Fig. 5[f]
Open ocean–coastal site									
Smith and Banke (1975)	0.053	0.16	0.27	0.99	0.952	8–21	Sable Island, Canada	T, EC	Table 1
Smith (1980)	0.055	0.25	0.19	0.95	0.927	8–22	Halifax Harbour	T, EC	Table 1
Large and Pond (1981)	0.049	0.16	0.23	0.95	0.995	8–19	Halifax Harbour	PV, ID	Fig. 3
Dobson et al. (1994)	0.050	0.13	0.27	0.97	0.927	8–17	Grand Banks	PV, ID	Table 1
Donelan et al. (1997)[g]	0.061	0.25	0.24	0.94	0.980	8–14	Virginia coast [Surface Wave Dynamics Experiment (SWADE)]	PV, ECM	Table 1
Drennan et al. (1999a)[g]	0.042	0.06	0.28	0.84	(−)0.977	8–17	Virginia coast (SWADE)	PV, ECM	Fig. 12a[h]
Sea/limited fetch									
Smith (1980)	0.044	0.06	0.29	0.96	(−)0.938	8–20	Halifax Harbour	T, EC	Table 2
Geernaert et al. (1987)	0.058	0.21	0.26	0.97	0.974	8–25	North Sea	S, EC	Table 2
Anderson (1993)	0.050	0.16	0.25	0.99	0.982	8–19	Georges Bank–Labrador Sea	PV, ID	Fig. 5a
Janssen (1997)	0.065	0.27	0.25	0.98	0.848	8–20	North Sea (HEXOS)	S, EC	Appendix A
Johnson et al. (1998)	0.047	0.10	0.27	0.97	0.852	8–16	Vindeby Island, Denmark (RASEX)	S, EC	Table 1
Bumke et al. (2002)	0.046	0.10	0.27	0.94	(−)0.982	8–15	Labrador Sea	S, ID	Fig. 7[i]
Larsen et al. (2003)[g]	0.049	0.13	0.26	0.94	0.942	8–17	Ostergarnsholm, Sweden	S, EC	Fig. 4c
Drennan et al. (2003)[g]	0.055	0.20	0.24	0.96	0.964	8–19	Gulf of Lion, Mediterranean [Flux, sea state, and remote sensing in conditions of variable fetch (FETCH)]	S, ECM	Fig. 4
Petersen and Renfrew (2009)	0.050	0.06	0.34	0.90	0.999	9–25	Denmark Strait [Greenland Flow Distortion Experiment (GFDex)]	A, ECA	Fig. 7a
Lake									
Graf and Prost (1980)	0.040	0.06	0.25	0.94	0.977	8–16	Lake Geneva	P	Table 1
Graf et al. (1984)	0.059	0.14	0.33	0.93	0.935	8–17	Lake Geneva	P	Table 2

Drennan et al. (1999b)	0.051[j]	0.11	0.30	0.83	1.000	8–16	Lake Ontario [Water–Air Vertical Exchange Study (WAVES)]	PV, EC	Fig. 4k
					Land (e.g.)				
Hicks (1976)	0.063[l]	−0.02	—	0.98	0.999	0–8	New South Wales, Australia (Wangara)	P	Fig. 1

[a] Wind speed range over which parameters C_m, b, u_{*_o}, etc. are calculated.
[b] Device indicated by S: sonic anemometer, PV: propeller–vane anemometer, T: thrust anemometer, and A: aircraft sensors; technique by EC: eddy correlation, ECM: eddy correlation with ship motion correction, ECA: high-altitude eddy correlation corrected after Donelan (1990), ID: inertial dissipation, and P: profile method.
[c] As found from within the referenced article.
[d] The near-perfect magnitude of R_{ns} (=1) here can be attributed to data that are both concave up (e.g., Large and Pond 1982) and concave down (e.g., Black et al. 2007).
[e] Only includes streamwise covariance stress.
[f] Hurricanes Edouard, Isadore, and Lili (2002); Fabian and Isabel (2003); and Frances and Jeanne (2004).
[g] Pure windsea data.
[h] Only includes data in stationary conditions.
[i] Only swell contaminated data could be extracted.
[j] Obtained from a drag coefficient based on a 12-m height.
[k] Includes windsea short and long fetch and mixed swell and wind wave.
[l] Found from a 0.5-m measurement height.

FIG. 2. The square root of the neutral drag coefficient here is interpreted as the slope of the u_* vs U_{10} distribution for $U_{10} \geq 8$ m s^{-1} and $u_* \geq 0.27$ m s^{-1}, and a straight line is fitted to data in this range. The HEXOS results as reported by Janssen (1997) are shown by triangles; the measurements of Anderson (1993) are indicated by squares.

that is approximately 12% of the mean. Previous estimates of α reported in the literature range from 0.01 over the open ocean (i.e., Smith 1988; Taylor and Yelland 2001) to approximately 0.02 over coastal sites or at high wind speeds (Yelland and Taylor 1996; Yelland et al. 1998; Fairall et al. 2003). Figure 3 shows that a Charnock's constant of $\alpha = 0.01$ (i.e., $u_{*_o} = 0.32$) gives $U_o = 9$ m s^{-1}, and hence the precise value of U_o will vary depending on α. If $\alpha = 0.01$ were to be assumed, then C_m in Eq. (12) moves from $C_m = 0.051$, based on $\alpha = 0.018$, to $C_m = 0.052$.

Shown in Fig. 4 is a plot showing the modified drag coefficient according to

$$u_* - u_{*_o} = C_m(U_{10} - U_o) \quad \text{for}$$
$$U_{10} \geq U_o, u_* \geq u_{*_o}\,\text{m s}^{-1}, \tag{13}$$

where $U_o = 8$ m s^{-1} and $u_{*_o} = 0.27$ m s^{-1}. It can be seen in this figure that the indirect proportionality resulting from the initial transition regime to rough flow has been removed.

c. *The difference between C_m and the standard definition of the drag coefficient C_D*

It has been suggested that the typical definition of the drag coefficient C_D reaches an upper limit for increasing U_{10} (e.g., Donelan et al. 2004), and Black et al. (2007) note the possible occurrence of this in their results. However, the tendency of C_D to increase with U_{10} and reach a limiting value is predominantly due to the neglect of the constant b.

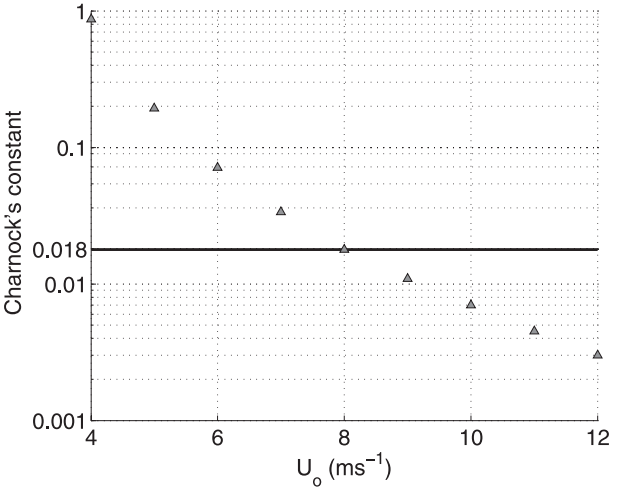

FIG. 3. Charnock's constant α as calculated from Eq. (7) by assuming various magnitudes of U_o. It can be seen that $U_o = 8$ m s^{-1} corresponds to $\alpha = 0.018$.

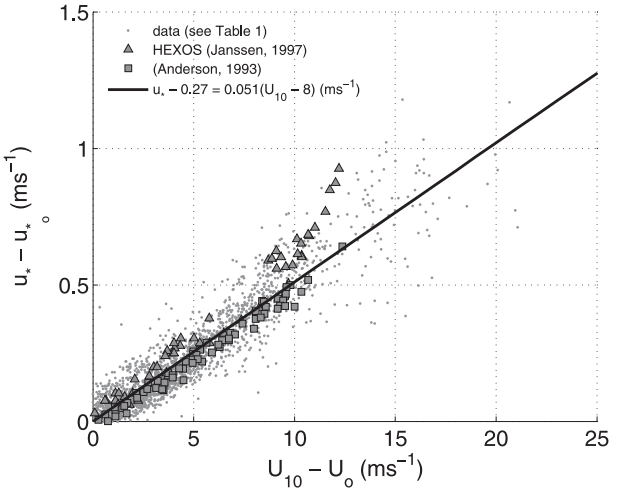

FIG. 4. Figure 2 plotted according to Eq. (13). Here the x and y axes are offset by $U_o = 8$ m s^{-1} and $u_{*_o} = 0.27$ m s^{-1}, respectively. The solid line is the line of best fit through this data, where the relationship is no longer offset from the origin.

This is perhaps clearer if it is realized that, according to Eq. (4), Fig. 1 (within the linear range) is actually a plot of

$$C_D = \frac{u_*^2}{U_{10}^2} = \frac{(U_{10}C_m + b)^2}{U_{10}^2} \tag{14}$$

against U_{10}. Therefore,

$$C_D = \frac{(U_{10}C_m + b)^2}{U_{10}^2} \rightarrow \frac{(U_{10}C_m)^2}{U_{10}^2} \tag{15}$$

as $U_{10} \rightarrow \infty$. Hence, as $U_{10} \rightarrow \infty$,

$$C_D \rightarrow C_m^2, \tag{16}$$

where an average of $C_m^2 = 0.0026$ is found according to all data collected in Table 1. Included in Fig. 1 is the drag coefficient given by Eq. (14) and the line $C_D \rightarrow C_m^2 = 0.051^2$ as found from our analysis, where the trend $C_D \rightarrow C_m^2$ is evident (either U_{10} needs to be significantly higher or b much smaller for $C_D \sim C_m^2$). This provides an upper limit to the magnitude of C_D and could be important with respect to the theoretical development of hurricanes (Emanuel 1995; Black et al. 2007).

d. Nonlinearity of $u_* = f(U_{10} - U_o)$

It has been assumed above that the linear regime exists for higher velocities ($U_{10} \geq U_o$ and $u_* \geq u_{*_o}$). With $U_o = 8$ m s^{-1} and $u_{*_o} = 0.27$ m s^{-1}, the nonlinearity of all data can be first tested by fitting a quadratic function giving

$$u_* = -0.000\,018U_{10}^2 + 0.051(U_{10} - 8) + 0.27, \tag{17}$$

which illustrates a weak nonlinearity within the range $8 < U_{10} < 30$ m s^{-1}. However, limiting the range of consideration to $8 < U_{10} < 20$ m s^{-1} gives

$$u_* = 0.0019U_{10}^2 + 0.033(U_{10} - 8) + 0.30, \tag{18}$$

where the nonlinear term here is more significant.

Therefore, to gauge the linearity in each individual dataset, shown in Table 1 are R_{ns} values, where R_{ns} is the ratio of the norm of residuals between a quadratic function and a linear function. The linear norm of residuals is

$$E_l = \left\{\sum[u_{*_i} - b - C_m(U_{10} - 8)]^2\right\}^{1/2}, \tag{19}$$

where u_{*_i} are measured and $b + C_m U_{10}$ are predicted friction velocities. Similarly, the quadratic norm of residuals is

$$E_q = \left\{\sum[u_{*_i} - a_2 - a_1(U_{10} - 8) - a_o(U_{10} - 8)^2]^2\right\}^{1/2}, \tag{20}$$

where a_o, a_1, and a_2 are quadratic model coefficients. The ratio between these norms of residuals is thus

$$R_{ns} = \frac{E_q}{E_l}. \tag{21}$$

For example, all data in Fig. 2 give $R_{ns} = 1.0000$ in the range $8 < U_{10} < 30$ m s^{-1} and $R_{ns} = 0.9708$ in the range $8 < U_{10} < 20$ m s^{-1}. The clearly nonlinear HEXOS results give $R_{ns} = 0.85$, whereas those of Anderson (1993)

give $R_{ns} = 0.98$. Values of R_{ns} are listed in Table 1, in addition to a negative sign in parentheses (−) if the quadratic function is concave down; for example, the HEXOS data is concave up and hence lacks a negative sign in Table 1. The near-perfect magnitude of R_{ns} (=1) here can be attributed to the contribution of data that are both concave up (e.g., Large and Pond 1982) and concave down (e.g., Black et al. 2007). In general, because $R_{ns} < 1$,[1] the linear model defined by Eq. (3) is an approximation. Table 1 shows that this is a good approximation for most data, which gives $R_{ns} \approx 1$. For other data, the assumption of linearity is weaker, and we believe this can be attributed to a lack of geometric similarity in regions of limited water depth.

For the drag coefficient to be constant,[2] geometric similarity at the very least must be maintained. For example, geometric similarity here is not maintained between low and high wind speeds (there is a surface roughness dependence), and hence the drag coefficient is not constant over this range. If geometric similarity is to be maintained at higher velocities, then a characteristic wave shape [let us suppose it is the wave steepness H/L, where H is some characteristic wave height (e.g., the significant wave height) and L a characteristic wavelength] must also be constant. For example, if the drag coefficient is to be constant for higher velocities, then H/L at 10 m s^{-1} must be the same H/L at 20 m s^{-1}. In deeper water, the wave shape at higher wind speeds is governed principally by the surface wind. A linear dependence of u_* on U_{10} at higher velocities suggests the forcing of the waves by the action of the surface wind at, for example, 10 and 20 m s^{-1} is equivalent and that geometric similarity is maintained in deeper water as a consequence of a persistent characteristic wave shape for increasing surface winds.

In the vicinity of a coast, in addition to the action of the wind, the characteristic wave shape can also be governed by sea floor effects (shoaling). It is possible that these two separate forcings combine to alter the characteristic wave shape so that now, for example, H/L at 10 m s^{-1} differs from H/L at 20 m s^{-1}, and hence the drag coefficient cannot be expected to be constant under these conditions. This is reflected in the magnitudes of $R_{ns} < 1$ in two particular datasets in Table 1 [HEXOS ($R_{ns} = 0.848$) and the Risø Air–Sea Experiment (RASEX) ($R_{ns} = 0.852$)] that also happen to be in regions of limited water depth. It is also consistent with the analysis of Taylor and Yelland (2001), who find a wave steepness dependence in both of these datasets. In these locations, the classical relationship as proposed by Charnock (1955), which predicts a nonlinear dependence of u_* on U_{10}, should be more valid than the linear relationship suggested here.

3. Conclusions

A reanalysis of the definition of the neutral drag coefficient in the marine boundary layer was conducted with the help of easily accessible data as reported in the literature. It is found that the increase in the drag coefficient with wind speed can be attributed to the neglect of a constant, a consequence of the friction velocity not being directly proportional to the mean wind speed. However, the friction velocity is still approximately linearly related to the mean wind speed at higher wind speeds. This linear regime is shown to be a feature of aerodynamically rough flow over water, similarly to that found over land, but the regime over water is offset from the origin by a transitional flow regime at low velocities. This offset justifies the introduction of the otherwise neglected constant b in Eq. (4).

An expression for the dependence of the friction velocity on the mean wind speed and Charnock's constant is found, which can be rearranged to form a new definition of the neutral drag coefficient in the marine atmospheric boundary layer, valid for a Charnock constant of 0.018 implying friction velocities greater than 0.27 m s^{-1} and wind speeds greater than 8 m s^{-1}. The new drag coefficient, C_m, approximates a range of datasets as reported in the literature for a range of locations including the open ocean, limited-fetch cases, as well as lakes, where the standard deviation is found to be approximately 12% of the mean. The square of the new drag coefficient turns out to be the limiting value for the classical drag coefficient for high wind speeds. The new drag coefficient is expected to be less valid in areas of limited water depth where the traditional definition in conjunction with Charnock's relation, which predicts a nonlinear dependence of u_* on U_{10}, such as that evident in the HEXOS data, is expected to be superior. In deeper water the new definition could prove to be useful, particularly at higher wind speeds.

Acknowledgments. We would like to acknowledge the efforts of two anonymous reviewers whose excellent feedback greatly improved this paper. This work was done within the VERITAS project (work package 5 of OWEA), which is funded by the German Ministry of the Environment (BMU) via the PTJ (FKZ 0325060).

[1] R_{ns} would get progressively lower if the numerator in Eq. (21) were to be calculated from the norm of residuals of a cubic, quartic, etc. function.

[2] In this context, a constant drag coefficient is assumed to be equivalent to a linear dependence of u_* on U_{10}.

REFERENCES

Anderson, R., 1993: A study of wind stress and heat flux over the open ocean by the inertial-dissipation method. *J. Phys. Oceanogr.,* **23,** 2153–2161.

Banner, M., W. Chen, E. J. Walsh, J. Jensen, S. Lee, and C. Fandry, 1999: The Southern Ocean Waves Experiment. Part I: Overview and mean results. *J. Phys. Oceanogr.,* **29,** 2130–2145.

Black, P., and Coauthors, 2007: Air–sea exchange in hurricanes: Synthesis of observations from the Coupled Boundary Layer Air–Sea Transfer experiment. *Bull. Amer. Meteor. Soc.,* **88,** 357–374.

Bumke, K., U. Karger, and K. Uhlig, 2002: Measurements of turbulent fluxes of momentum and sensible heat over the Labrador Sea. *J. Phys. Oceanogr.,* **32,** 401–410.

Charnock, H., 1955: Wind stress on a water surface. *Quart. J. Roy. Meteor. Soc.,* **81,** 639–640.

Davidson, K., 1974: Observational results on the influence of stability and wind-wave coupling on momentum transfer and turbulent fluctuations over ocean waves. *Bound.-Layer Meteor.,* **6,** 305–331.

Dobson, F., S. Smith, and R. Anderson, 1994: Measuring the relationship between wind stress and sea state in the open ocean in the presence of swell. *Atmos.–Ocean,* **32,** 237–256.

Donelan, M. A., 1990: Air–sea interaction. *The Sea,* B. LeMehaute and D. M. Hanes, Eds., *Ocean Engineering Science,* Vol. 9, John Wiley and Sons, 239–292.

——, W. M. Drennan, and K. B. Katsaros, 1997: The air–sea momentum flux in conditions of wind sea and swell. *J. Phys. Oceanogr.,* **27,** 2087–2099.

——, B. Haus, N. Reul, W. Plant, M. Stiassnie, H. Graber, O. Brown, and E. Saltzman, 2004: On the limiting aerodynamic roughness of the ocean in very strong winds. *Geophys. Res. Lett.,* **31,** L18306, doi:10.1029/2004GL019460.

Drennan, W. M., H. C. Graber, and M. A. Donelan, 1999a: Evidence for the effects of swell and unsteady winds on marine wind stress. *J. Phys. Oceanogr.,* **29,** 1853–1864.

——, K. K. Kahma, and M. A. Donelan, 1999b: On momentum flux and velocity spectra over waves. *Bound.-Layer Meteor.,* **92,** 489–515.

——, H. C. Graber, D. Hauser, and C. Quentin, 2003: On the wave age dependence of wind stress over pure wind seas. *J. Geophys. Res.,* **108,** 8062, doi:10.1029/2000JC000715.

Emanuel, K., 1995: Sensitivity of tropical cyclones to surface exchange coefficients and a revised steady-state model incorporating eye dynamics. *J. Atmos. Sci.,* **52,** 3969–3976.

Fairall, C. W., E. F. Bradley, D. P. Rogers, J. B. Edson, and G. S. Young, 1996: Bulk parameterization of air-sea fluxes for Tropical Ocean-Global Atmosphere Coupled-Ocean Atmosphere Response Experiment. *J. Geophys. Res.,* **101** (C2), 3747–3764.

——, ——, J. E. Hare, A. A. Grachev, and J. B. Edson, 2003: Bulk parameterization of air–sea fluxes: Updates and verification for the COARE algorithm. *J. Climate,* **16,** 571–591.

Garratt, J., 1977: Review of drag coefficients over oceans and continents. *Mon. Wea. Rev.,* **105,** 915–929.

Geernaert, G., 1990: Bulk parameterizations for the wind stress and heat fluxes. *Surface Waves and Fluxes,* Kluwer Academic, 91–172.

——, S. Larsen, and F. Hansen, 1987: Measurements of the wind stress, heat flux, and turbulence intensity during storm conditions over the North Sea. *J. Geophys. Res.,* **92,** 13 127–13 139.

Graf, W. H., and J. P. Prost, 1980: Aerodynamic drag and its relation to the sea state: With data from Lake Geneva. *Meteor. Atmos. Phys.,* **29,** 67–87.

——, N. Merzi, and C. Perrinjaquet, 1984: Aerodynamic drag: Measured at a nearshore platform on Lake of Geneva. *Meteor. Atmos. Phys.,* **33,** 151–173.

Hasse, L., and S. Smith, 1997: Local sea surface wind, wind stress, and sensible and latent heat fluxes. *J. Climate,* **10,** 2711–2724.

Hicks, B., 1976: Wind profile relationships from the 'Wangara' experiment. *Quart. J. Roy. Meteor. Soc.,* **102,** 535–551.

Hsu, S., 1974: A dynamic roughness equation and its application to wind stress determination at the air-sea interface. *J. Phys. Oceanogr.,* **4,** 116–120.

Janssen, J. A. M., 1997: Does the wind stress depend on sea-state or not? A statistical error analysis of HEXMAX data. *Bound.-Layer Meteor.,* **83,** 479–503.

Johnson, H., J. Hojstrup, H. Vested, and S. Larsen, 1998: On the dependence of sea surface roughness on wind waves. *J. Phys. Oceanogr.,* **28,** 1702–1716.

Lange, B., H. Johnson, S. Larsen, J. Hojstrup, H. Kofoed-Hansen, and M. Yelland, 2004: On the detection of a wave age dependency for the sea surface roughness. *J. Phys. Oceanogr.,* **34,** 1441–1458.

Large, W., and S. Pond, 1981: Open ocean momentum flux measurements in moderate to strong winds. *J. Phys. Oceanogr.,* **11,** 324–336.

——, and ——, 1982: Sensible and latent heat flux measurements over the ocean. *J. Phys. Oceanogr.,* **12,** 464–482.

Larsen, X., V. Makin, and A. Smedman, 2003: Impact of waves on the sea drag: Measurements in the Baltic Sea and a model interpretation. *J. Atmos. Ocean Sci.,* **9,** 97–120.

Maat, N., C. Kraan, and W. Oost, 1991: The roughness of wind waves. *Bound.-Layer Meteor.,* **54,** 89–103.

Oost, W., G. Komen, C. Jacobs, and C. V. Oort, 2002: New evidence for a relation between wind stress and wave age from measurements during ASGAMAGE. *Bound.-Layer Meteor.,* **103,** 409–438.

Persson, P., J. Hare, C. Fairall, and W. Otto, 2005: Air-sea interaction processes in warm and cold sectors of extratropical cyclonic storms observed during FASTEX. *Quart. J. Roy. Meteor. Soc.,* **131,** 877–912.

Petersen, G., and I. Renfrew, 2009: Aircraft-based observations of air-sea fluxes over Denmark Strait and the Irminger Sea during high wind speed conditions. *Quart. J. Roy. Meteor. Soc.,* **135,** 1950–1967, doi:10.1002/qj.455.

Smith, S., 1980: Wind stress and heat flux over the ocean in gale force winds. *J. Phys. Oceanogr.,* **10,** 709–726.

——, 1988: Coefficients for sea surface wind stress, heat flux, and wind profiles as a function of wind speed and temperature. *J. Geophys. Res.,* **93** (C12), 15 467–15 472.

——, and E. Banke, 1975: Variation of the sea surface drag coefficient with wind speed. *Quart. J. Roy. Meteor. Soc.,* **101,** 665–673.

——, and Coauthors, 1992: Sea surface wind stress and drag coefficients: The HEXOS results. *Bound.-Layer Meteor.,* **60,** 109–142.

Stull, R. B., 1988: *An Introduction to Boundary Layer Meteorology*. Kluwer Academic, 666 pp.

Sullivan, P., and J. McWilliams, 2010: Dynamics of winds and currents coupled to surface waves. *Annu. Rev. Fluid Mech.,* **42,** 19–42.

Taylor, P., and M. Yelland, 2001: The dependence of sea surface roughness on the height and steepness of the waves. *J. Phys. Oceanogr.,* **31,** 572–590.

Wu, J., 1980: Wind-stress coefficients over sea surface near neutral conditions—A revisit. *J. Phys. Oceanogr.,* **10,** 727–740.

Yelland, M., and P. Taylor, 1996: Wind stress measurements from the open ocean. *J. Phys. Oceanogr.,* **26,** 541–558.

——, B. Moat, P. Taylor, R. Pascal, J. Hutchings, and V. Cornell, 1998: Wind stress measurements from the open ocean corrected for airflow distortion by the ship. *J. Phys. Oceanogr.,* **28,** 1511–1526.